Theor Chem Acc (2003) 109:316–325
DOI 10.1007/s00214-003-0431-9

Theoretical
Chemistry Accounts

Regular article

Nature of interaction energy anisotropy in the Li(^{2}S)–HF ($\tilde{X}^1\Sigma^+$) van der Waals complex. A theoretical study

Vladimír Lukeš[1], **Martina Bittererová**[2], **Stanislav Biskupič**[2], **Viliam Laurinc**[1]

[1] Department of Chemical Physics, Slovak University of Technology, Radlinského 9, 812 37 Bratislava, Slovak Republic
[2] Department of Physical Chemistry, Slovak University of Technology, Radlinského 9, 812 37 Bratislava, Slovak Republic

Received: 10 May 2002 / Accepted: 19 December 2002 / Published online: 20 May 2003

Abstract. The potential-energy surface for the Li(^{2}S)–HF ($\tilde{X}^1\Sigma^+$) interaction, where HF is kept rigid, is calculated using the supermolecular unrestricted fourth-order Møller–Plesset perturbation theory. The basis set superposition error corrected potential indicates two minima. The global minimum occurs for the bent Li...FH structure at $R = 1.95$ Å and $\theta = 70°$ with a relatively deep well of $D_e = 1{,}706$ cm^{-1} and the secondary minimum is found for the linear Li...HF configuration at $R = 4.11$ Å with a well depth of $D_e = 288$ cm^{-1}. A barrier of 177 cm^{-1} (with respect to the secondary linear minimum) separates these two minima. In this study 27 bound states of the bent Li...FH minimum and eight bound states of the linear Li...HF minimum up to the Li + HF dissociation threshold are calculated. The energy partitioning using the intermolecular perturbation theory scheme shows that the origins of the stability of the structures studied are entirely different. The global minimum is stabilised using the attractive Coulombic interaction and unrestricted Hartree–Fock deformation energy. The latter term originates from the mutual electric polarisation effects. The secondary linear minimum is mostly determined by the anisotropy of the repulsive Heitler–London exchange-penetration and attractive dispersion energies.

Keywords: Potential-energy surface – Li–HF – Bound states – Weak interaction – Intermolecular perturbation theory

Introduction

One of the ongoing challenges in the study of intermolecular forces is to gain insight into the nature of open-shell van der Waals (vdW) complexes [1, 2, 3, 4]. There is growing interest in these systems for three reasons: their interactions are viewed as intermediate between nonbonding vdW interactions and the chemical bonding; many of them are prereactive complexes formed in the entrance valleys of potential-energy surface (PES); and the presence of unpaired electrons might induce a new type of electronic anisotropy. Open-shell vdW molecules can affect the outcome of reactive events, as well. The remote regions of the reactive PES are governed by the long-range forces. These forces possess the capacity for orienting the reactants favourably or unfavourably as they approach one another or may trap them in potential wells, before they have a chance to engage in reactive encounters.

A number of experiments have been performed on the Li + HF → LiF + H reaction as a prototype of a heavy–heavy–light system, becoming a benchmark in molecular reaction dynamics owing to its relative simplicity [5, 6, 7, 8, 9]. The diatomic fragments having strong dipolar moments allow the preparation of reagents in specific initial states and the determination of the final state of products. In addition, the reagents present a sufficiently deep well in the entrance channel from which the system can be excited and the reaction dynamics studied at very precise energies [10].

Earlier molecular beam studies [5] cannot be used to extract information about the spectroscopy of the Li...HF precursor complex. The experimental work that offers some basic and reliable facts about this weak interaction is the nonreactive scattering experiment by Loesh and Stienkemeier [6, 7]. Their experiment provides evidence of a well depth of 300 meV (2,420 cm^{-1}). This finding is not in disagreement with the theoretical results obtained at the various ab initio calculation levels [10, 11, 12]. For example, the full optimised PES of Jasper et al. [11] based on the MRDCI method has the minimum at $\theta_{Li–F–H} = 110°$, $R_{LiF} = 1.88$ Å, with interaction energy −0.211 eV (–1,702 cm^{-1}). The optimised geometry of the interact-

Correspondence to: Viliam Laurinc
e-mail: laurinc@cvt.stuba.sk

ing HF molecule was changed minimally (prolongation about 0.01 Å) with respect to the equilibrium distance. The basis set superposition error (BSSE) [13] corrected CCSD(T) calculations [12] based on the unrestricted Hartree–Fock (UHF) single-determinant reference are not in contradiction with conclusions of the work mentioned previously.

The contour map of the ab initio PES (MRDCI calculations without BSSE corrections) of Aguado et al. (HF distance fixed at 0.921 Å, see Fig. 2 in Ref. [10]) shows two minima, the global minimum at $\theta = 107°$ and a less deep minimum for a linear Li...HF arrangement at an energy of about −0.08 eV. Very recently the first observation of the Li...HF complex was reported and theoretically interpreted by Hudson et al. [8]. To the best of our knowledge, no preliminary information on spectroscopic characteristics of the secondary linear Li...HF vdW complex is available.

The ab initio PESs of the LiHF system presented in the literature were evaluated using the supermolecular (SM) approach. Although the SM approach is conceptually and computationally simple, it cannot offer a clear picture of interaction forces. On the other hand, the intermolecular perturbation theory (I-PT) allows direct calculations of electrostatic, exchange-penetration, dispersion and induction contributions that provide a physical interpretation of the interactions between the monomers of a complex. The applicability of I-PT based on the single-determinant restricted Hartree–Fock or UHF reference wave functions has recently been presented for several open-shell vdW systems [14, 15, 16, 17].

The purpose of the present study is to provide the BSSE-free characterisation of the PES with respect to the linear vdW minimum at the SM unrestricted fourth-order Møller–Plesset (UMP4) theoretical level. The PES is fitted to the analytical form and used to calculate vibrational energy levels of the LiHF system. Finally, using the I-PT analysis of the UMP results, we discuss the physical background of interaction energy anisotropy and individual energy contributions are visualised by the contour diagrams.

Methodology and definitions

In order to investigate the weak interaction within the open-shell vdW system, we use the standard ab initio SM approach. At a given level of perturbation theory, the interaction energy is calculated from the expression

$$\Delta E_{\mathrm{int}}^{(n)} = E_{\mathrm{AB}}^{(n)} - E_{\mathrm{A}}^{(n)} - E_{\mathrm{B}}^{(n)} \quad n = \mathrm{UHF}, 2, 3, 4, \ldots, \tag{1}$$

where E_{AB} is the energy of the supersystem AB, and E_{A} (E_{B}) denotes the energy of the noninteracting monomer A (B). The level of theory is indicated by the superscript index n, for example, $\Delta E_{\mathrm{int}}^{(2)}$ denotes the UMP2 interaction energy.

The UHF–self-consistent-field (SCF) interaction energy can be decomposed as follows:

$$\Delta E^{\mathrm{UHF}} = \Delta E^{\mathrm{HL}} + \Delta E_{\mathrm{def}}^{\mathrm{UHF}}, \tag{2}$$

where ΔE^{HL} is the Heitler–London (HL) energy [18] and $\Delta E_{\mathrm{def}}^{\mathrm{UHF}}$ represents the UHF deformation contribution [2, 3]. According to the I-PT defined in the orthogonalised basis sets [18, 19], ΔE^{HL} may be further divided into the first-order Hartree–Fock electrostatic term, $E_{\mathrm{els}}^{(100)}$ (for the notation for this term and further perturbation terms see e.g. Ref. [20]), and HL exchange-penetration term, $\Delta E_{\mathrm{exch}}^{\mathrm{HL}}$:

$$\Delta E^{\mathrm{HL}} = \Delta E_{\mathrm{exch}}^{\mathrm{HL}} + E_{\mathrm{els}}^{(100)}. \tag{3}$$

The UHF deformation energy originates from the mutual electric polarisation effects. This term might be approximated using the sum of the following two perturbation terms: $E_{\mathrm{ind}}^{(200)}$ and $E_{\mathrm{exch-ind}}^{(200)}$ (second-order UHF Coulomb and exchange-induction energies) [21]. However, the inclusion of the higher-order perturbation contributions and the response or orbital-relaxation effects is necessary at shorter intermolecular distances [3, 20, 21].

Similarly to the closed-shell cases, the UMP2 correlation interaction energy can be partitioned as

$$\Delta E_{\mathrm{int}}^{(2)} = E_{\mathrm{els}}^{(12)} + E_{\mathrm{disp}}^{(200)} + E_{\mathrm{exch-disp}}^{(200)} + \Delta E_{\mathrm{other}}^{(2)}, \tag{4}$$

where $E_{\mathrm{els}}^{(12)}$ denotes the second-order electrostatic correlation energy (containing $E_{\mathrm{els}}^{(102)}$ and $E_{\mathrm{els}}^{(120)}$ energies). $E_{\mathrm{disp}}^{(200)}$ and $E_{\mathrm{exch-disp}}^{(200)}$ represent the second-order Hartree–Fock dispersion [22] and exchange-dispersion energies [20]. $\Delta E_{\mathrm{other}}^{(2)}$ encompasses the remaining exchange and deformation correlation corrections as well as the response effects [2, 3].

Using diagrammatic techniques, it is possible to distinguish the third-order interaction energy contributions, like the dispersion-correlation ($E_{\mathrm{disp}}^{(210)}$, $E_{\mathrm{disp}}^{(201)}$) and Hartree–Fock third-order dispersion ($E_{\mathrm{disp}}^{(300)}$) energies [15, 20]. However, the complete physical interpretation of the higher-than-second-order contributions of the interaction electron-correlation energies is not straightforward.

To test the stability of the linear vdW complex, vibrational energy levels were calculated. We used the standard body-fixed Hamiltonian in atom–diatom Jacobi coordinates. Let us denote the HF internuclear distance by r, the distance from the centre of mass of HF to Li by R, and the angle between vectors r and R by θ, where $\theta = 180°$ corresponds to a linear LiHF arrangement. Coriolis coupling is small in the case of LiHF [12]. In this work, we focus on the rotationless ($J = k = 0$) eigenstates of the Hamiltonian.

The total angular momentum zero ($J = 0$) Hamiltonian is

$$\hat{H} = -\frac{1}{2\mu}\frac{\partial^2}{\partial R^2} - \frac{1}{2\mu_{\mathrm{HF}}}\frac{\partial^2}{\partial r^2} + \left(\frac{1}{2\mu R^2} + \frac{1}{2\mu_{\mathrm{HF}} r^2}\right)\hat{j}^2 + V(r, R, \theta), \tag{5}$$

where μ and μ_{HF} are the reduced masses of Li–HF and HF, respectively, and where $\hat{j}^2$ is the angular momentum operator for HF.

Calculation details

The PES calculations were performed using the UMP4 method. All UMP4 energies were corrected for the effects of the BSSE in the Li...FH complex. I-PT calculations were performed by our own program codes interfaced to the Gaussian 94 program package [23]. The SM BSSE was determined via the counterpoise method of Boys and Bernardi [24]. The presented UHF interaction energy terms were developed using dimer-centred basis sets of the constituent monomers [13]. The evaluation of the second-order exchange-induction and exchange-dispersion energies at the UHF level was realised in the framework of the single-exchange approximation [20]. The HL energy was

obtained using the standard Gram–Schmidt orthogonalisation procedure.

The augmented correlation consistent basis set aug-cc-pVTZ [25, 26] was used for hydrogen and fluorine atoms. Owing to the fact that augmented basis sets for the Li atom were not available, we decided to use the basis set reported by Sadlej [27]. It represents the near triple-ζ quality basis set augmented by the polarisation functions suitably optimised to reproduce the molecular electric properties, especially polarisabilities.

The bound-state energies were determined by a simple, grid-based, iterative technique as implemented in the ROVIB3 program [28, 29, 30]. For the case of triatomic systems of the type A...BC, the "fast" vibrational motion of BC can be decoupled from the "slow" intermolecular motions of A...BC [31]. In a previous study of the Li...FH vdW complex [12] it was shown that the two-dimensional model, which completely neglects the coupling between the high- and low-frequency motions, provides a satisfactory description of the vibrational levels. In our work we perform interaction energy calculations within the two-dimensional model assuming the HF distance fixed at its equilibrium value, r_e. In order to use the three-dimensional variational approach for the vibrational states of Li...HF as implemented in the ROVIB3 program package, the PES $V(r, R, \theta)$ is written as a sum of $V_{BC}(r)$, the intramolecular potential interaction of the free diatomic molecule HF, and $V(R, \theta)$, the intermolecular interaction between the A and BC diatomic molecule. $V(R, \theta)$ is fitted to the analytical form and the $V_{BC}(r)$ potential is approximated by the Morse potential $V_{BC}(r) = D_e\{1 - \exp[-\beta_e(r - r_e)]\}^2$. The Morse parameters are taken from experiment [32]. Thus, we have $V(r) \to 0$ as $r \to \infty$. At large R distances between atom A and the centre of mass of the BC molecule $V(r, R, \theta) \to V(r)$. Application of this approach leads to a considerable simplification of the intermolecular PES computation. In the vicinity of the linear stationary point the differences between the ab initio and fitted energies are less than 2 cm^{-1}.

The Hamiltonian matrix and associated wave functions are represented with evenly spaced grids or discrete variable representations (DVRs) [33, 34] in R and r, and associated Legendre polynomials to describe $\cos\theta$. The wave function is an expansion in the associated Legendre polynomials, with the expansion coefficients depending on R and r. The action of the Hamiltonian matrix on a vector is similar to that discussed in Refs. [28, 29], except that r is now treated just like R with an evenly spaced DVR. As such, the corresponding problem dimension can be large, so it is possible to apply energetic cutoffs within a DVR by excluding those DVR points that yield potential energies greater than some cutoff value E_{cut} (potential-optimized DVRs [35, 36]). In this work we use $E_{cut} = 13{,}170$ cm^{-1} that is above the energies of interest. To determine vibrational eigenstates and the corresponding eigenvectors, we employed the implicitly restarted Lanczos (or more generally Arnoldi) method as implemented in the ARPACK software package [37].[1]

Results and discussion

Features of the UMP4 PES

The two-dimensional PES of the ground electronic state of the Li...FH vdW complex was calculated in the range of R from 1.6 to 8 Å and θ from 0 to 180°, while r was fixed at the equilibrium HF distance, 0.9168 Å [32]. The calculated potential-energy points were fitted to the following general functional form

$$V(R,\theta) = V_{\max}\left(\sum_{L=0}^{7}\sum_{k=0}^{6} a_k^L\{\exp[-a_1(R-a_2)]\}^k \times P_L^0(\cos\theta) + 1\right),$$

where the energies are given in μE_h and $P_L^0(\cos\theta)$ denote Legendre polynomials up to order $L = 7$. A rigorous least-squares fitting procedure based on the singular value decomposition was used to determine all 58 variational parameters (Table 1—the Fortran code is available on the request). Prior to the least-squares calculation, the original grid of 360 potential-energy points was expanded by the bicubic spline interpolation procedure [38] to 3,293 points. The average absolute deviation between the original points and the fit was smaller than 7.5 μE_h (1.6 cm^{-1}). In addition to the recent CCSD(T) study of the Li...FH bound states [12], in this work we investigate the properties of the secondary linear Li...HF vdW minimum.

The energies are given on an energy scale such that Li + HF, with HF at its asymptotic equilibrium geometry ($r = 0.9168$ Å), is the zero energy. The evaluated PES reveals three stationary points. The potential-energy minimum is a bent LiFH vdW structure with potential energy –7,775 μE_h (−0.212 eV or −1,706 cm^{-1}), while the CCSD(T) potential energy minimum lies at –1,991 cm^{-1}. The differences between the dissociation energies characterising the Li...FH vdW complex are large because the minimum is located close to the repulsive part of the PES. A secondary linear Li...HF vdW

[1] ARPACK is a program package designed to solve large-scale eigenvalue problems. The package is designed to compute a few eigenvalues and corresponding eigenvectors of a general $n \times n$ matrix **A**. This software is based upon an algorithmic variant of the Arnoldi process called the implicitly restarted Arnoldi method. When the matrix **A** is symmetric it reduces to a variant of the Lanczos process called the implicitly restarted Lanczos method. ARPACK software is capable of solving large-scale symmetric, nonsymmetric, and generalized eigenproblems from significant application areas. The software is designed to compute a few (k) eigenvalues with user specified features such as those of largest real part or largest magnitude. Storage requirements are on the order of $n*k$ locations. See the ARPACK homepage, http://www.caam.rice.edu/software/ARPACK

Table 1. Parameters of the analytical potential (Eq. 1)($V_{max} = 296{,}092.1\ \mu E_h, a_1 = 1.18571521\ Å^{-1}, a_2 = 2.06676866\ Å$)

L	a_2^L	a_3^L	a_4^L	a_5^L	a_6^L	a_7^L	a_8^L
0	−1.00016926	$-0.267038604\times10^{-1}$	0.121399790	−0.188902029	0.139563401	$-0.357344469\times10^{-1}$	0.257031498×10^{-2}
1	$-0.639346620\times10^{-4}$	0.269899155×10^{-1}	−0.208710656	0.210033428	−0.160377698	0.643948856×10^{-1}	$-0.109587441\times10^{-1}$
2	0.126164779×10^{-3}	$-0.323903055\times10^{-1}$	0.228296752	−0.256053611	0.228858903	−0.109166421	0.220638475×10^{-1}
3	0.243331995×10^{-5}	0.132440744×10^{-1}	$-0.698213005\times10^{-1}$	$-0.148883394\times10^{-1}$	0.634548123×10^{-1}	$-0.536540044\times10^{-1}$	0.131287590×10^{-1}
4	$-0.424960667\times10^{-4}$	$-0.251755289\times10^{-2}$	0.106208110×10^{-1}	0.758331115×10^{-1}	-0.115779947	0.766760118×10^{-1}	$-0.174376205\times10^{-1}$
5	$-0.118904510\times10^{-3}$	0.649452966×10^{-2}	$-0.561560721\times10^{-1}$	0.136480586	-0.187866955	0.114258585	$-0.260859578\times10^{-1}$
6	0.334620638×10^{-4}	$-0.157991256\times10^{-2}$	0.159084070×10^{-1}	$-0.468306904\times10^{-1}$	0.749276481×10^{-1}	$-0.500363626\times10^{-1}$	0.123164388×10^{-1}
7	0.959552915×10^{-4}	$-0.443029085\times10^{-2}$	0.365030953×10^{-1}	−0.106723325	0.135488304	$-0.785015781\times10^{-1}$	0.167294866×10^{-1}

minimum exists at $R = 4.11$ Å with an energy of –1,314 μE_h (−0.036 eV or –288 cm^{-1}). The MRDCI calculations [10] reveal the same position of the linear stationary point. The transition state between the bent and linear forms has a potential energy of –503.6 μE_h. (The barrier height relative to the linear minimum is 810.4 μE_h.)

The geometries, harmonic frequencies and zero-point energies of the stationary points of the analytical LiHF surface are listed in Table 2. The harmonic frequencies and zero-point energies were calculated by treating the HF vibrational mode as decoupled from the other modes. For the ground-state geometry the agreement with recent calculations [11] is reasonable. The LiF and LiH distances calculated within the two-dimensional model are about 0.05 Å longer than the MRDCI distances [11] obtained from the fully dimensional PES.

The values of dissociation energy (D_e) characterizing the global minimum on the PES, the Li...FH vdW complex predicted previously, vary from 1,605 cm^{-1} (CISD) [39] to 2,250 cm^{-1} (MRDCI) [10]. The experimental estimate of $D_e = 2{,}420\ cm^{-1}$ obtained from backward glory scattering [7] is according to the authors somewhat too large (by about 25%). Our BSSE-corrected UMP4 value of 1,706 cm^{-1} is in very good agreement with the recently reported MRDCI value, 1,702 cm^{-1} [11].

Within the SM approach, the truncation effect of the correlation treatment on the values of the interaction energies is significant and strongly dependent on R and θ. Individual contributions to the interaction energies of the LiHF stationary points are given in Table 3. The HF interaction energy (ΔE^{UHF}) represents a very important attractive contribution around the first minimum. The dominant part of the interaction correlation energy naturally originates from the values computed at the UMP2 level of theory. Although the higher-order contributions to the correlation energy $\Delta E^{(3)}$ ($\Delta E^{(3)}_{int} - \Delta E^{(2)}_{int}$) and $\Delta E^{(4)}$ ($\Delta E^{(4)}_{int} - \Delta E^{(3)}_{int}$) are smaller than $\Delta E^{(2)}$, they affect the value of the interaction energy. The interaction energies calculated using the CCSD(T) method within the same basis set appear to be lower (about 3.2–8.0%) than UMP4 values. Finally we would like to note that in

Table 2. Equilibrium structure (Å, degrees), harmonic vibrational frequencies, zero-point energies (*ZPEs*), and relative energies (cm^{-1}) for the LiHF stationary points [$R_{HF} = 0.9168$ Å, ω_1 (HF stretch) = 4,138 cm^{-1}]

Stationary point	Global minimum	Transition state	Linear minimum
R_{LiF}	1.936	3.677	4.159
$\alpha_{Li\text{-}F\text{-}H}$	108.5	65.3	0
V_1[a]	−1,706	−111	−288
V_1 + ZPE	760	1,991	1,974
ω_2	367 (A′)	−109 (A′)	70 (Σ^+)
ω_3	425 (A′)	65 (A′)	158 (Π)
ZPE	2,466	2,102	2,262

[a]Energies are given relative to the Li + HF dissociation limit

Table 3. Individual contributions to the interaction energy (cm^{-1}) of the Li(^{2}S)–HF ($\tilde{X}^1\Sigma^+$)complex

Geometry	$R=1.95$ Å $\theta=70°$	$R=3.64$ Å $\theta=113°$	$R=4.11$ Å $\theta=180°$
ΔE^{UHF}	−1,248.2	145.2	−1.8
$\Delta E^{(2)}$	−323.8	−206.4	−240.2
$\Delta E^{(2)}_{int}$	−1,572.0	−61.2	−242.0
$\Delta E^{(3)}$	−115.9	−4.7	0.4
$\Delta E^{(3)}_{int}$	−1,687.9	−65.9	−241.6
$\Delta E^{(4)}$	7.3	−43.6	−48.6
$\Delta E^{(4)}_{int}$	−1,680.6	−109.5	−290.2
$\Delta E^{CCSD(T)}_{int}$	−1,810.6	−121.2	−299.8
ΔE^{HL}	3,340.2	423.7	461.6
$E^{(100)}_{els}$	−10,825.1	−432.8	−5.0
ΔE^{UHF}_{def}	−4,588.4	−278.5	−463.4
$E^{(200)}_{ind}$	−19,889.3	−1,000.8	−603.7
$E^{(200)}_{exch-ind}$	18,338.4	955.1	462.0
$E^{(12)}_{els}$	−89.9	−49.1	−29.3
$E^{(200)}_{disp}$	−2825.5	−310.1	−199.0
$E^{(200)}_{exch-disp}$	1,476.5	108.0	50.5
$\Delta E^{(2)}_{other}$	1,115.1	44.7	−62.5
$E^{(210)}_{disp}+E^{(201)}_{disp}$	72.1	−20.1	−21.0
$E^{(300)}_{disp}$	59.0	9.7	11.8
E_{disp}	−1,217.9	−212.5	−157.7

all cases the spin contamination was negligible because $<S^2>=0.750$ corresponds to the exact value in the radical monomer as well as the dimer.

Bound states

Vibrational levels were calculated up to the Li + HF dissociation threshold (2,045 cm^{-1}). After some test calculations we chose the basis set of 127 functions on the grid from $2.7a_0$ to $12.0a_0$ (1.43–6.35 Å), 59 functions for r on the grid from $1.3a_0$ to $2.3a_0$ (0.69–1.22 Å), and 60 basis functions for $\cos\theta$ on the grid from –1 to 1, corresponding to θ between 0 and 180°. Three-dimensional grid points with energies larger than 13,170 cm^{-1} were discarded, resulting in a final matrix size of 450,000. In order to estimate bound states of the linear local minimum, we also used the smaller R-box. The R parameters varied between $6.0a_0$ and $14.0a_0$ (3.17–7.41 Å) with a $0.073a_0$ (0.039 Å) step, while the other boxing parameters remained the same. In this case the matrix size was about 39,000.

The accuracy of the energy levels was estimated by additional calculations with slightly different ranges and grid point numbers. With these parameters, the energy levels agreed within 1 cm^{-1}.

The topological features of the PES suggest that some interesting level patterns may arise for higher energies, especially energies in the vicinity of the linear local minimum on the surface. We determined the lowest 27 ($J=0$) vibrational states for the $\tilde{X}(1^2A')$ LiHF state. This represents vibrational energies up to $E\approx$ 2,040 cm^{-1}. In Table 4 the vibrational eigenvalues of the Li...FH ground electronic state and the linear local minimum are listed and compared to the relevant results reported previously [9, 12].

The effect of the zero-point oscillation is clearly large. The harmonic zero-point energy of the ground electronic state and the linear local minimum were calculated to be 2,466 and 2,262 cm^{-1}. The zero-point energies predicted by the bound state calculations are 2,404 and 2,202 cm^{-1}, respectively.

Vibronic wave functions for the states below the dissociation energy were calculated and analysed. Each wave function was visually inspected by a two-dimensional plotting routine in order to assign quantum numbers. Contour maps of selected eigenfunctions in Jacobi coordinates R and θ, while r is fixed at 0.9168 Å, are displayed in Fig. 1. (The corresponding eigenvalues are given in Table 4). Sometimes the wave functions are not aligned along any of the three planes, so we considered all three planes: (R, r), (R, θ), and (r, θ).

The ordering of the lowest seven states is the same as in work of Paniagua [9] except for states (0,0,2) and (0,1,1). For excited vibrational states, the agreement with the CCSD(T) results [12] is worse. Usually, the states obtained in our calculations lie systematically lower than the states obtained by CCSD(T) calculations [12]. Up to an energy of about 1,900 cm^{-1} all states can be unambiguously assigned to the LiHF ground electronic state. As the energy increases, the secondary minimum perturbs the shape of the wave function and does not allow a clear-cut assignment.

In the linear minimum case, the vibrational energy levels were obtained from the bound-state calculations based on the smaller R-box. A linear local minimum series starts at $E=1{,}914$ cm^{-1} which basically corresponds to the 17th state calculated in the big R box. The wave function of the 17th state is shown in Fig. 1 (17). This wave function is mostly localized around $\theta\approx180°$. There is a very shallow barrier between the global minimum and the linear local minimum; therefore the wave function tunnels through the barrier and is localised with much smaller intensity on the global minimum, as well. State 18 with energy 1,925 cm^{-1} is assigned to the global minimum as (0,1,3). This state is not perturbed by the linear local minimum. Figure 1 (19, 20) shows very diffuse wave functions that can be associated with both minima on the PES. It would be interesting to observe states of the mixed global/local minimum character.

Our calculations illustrate that the series for the local linear minimum actually interfuse among other levels of the global minimum. Because the global minimum of the PES is at $\theta=70°$, we expect that the lowest energy states will be the ones that have the largest probability at $\theta=70°$. However, at energies above 1,900 cm^{-1} states will concentrate around the linear configuration (Li...HF) as well.

Table 4. Vibrational energy levels (cm^{-1})for LiHF, (*A*) the ground electronic state $\tilde{X}(1^2A')$,(*B*) the Li...HF linear local minimum ($^2\Sigma^+$)

No.	A					No.	B[d]		
	Energy[a]	(v_r,v_R,v_θ)	This work	CCSD(T)[b]	MRDCI[c]		Energy[a]	(v_r,v_R,v_θ)	This work
1	698	(0,0,0)	0						
2	1,003	(0,1,0)	305	322.3	363.2				
3	1,024	(0,0,1)	326	363.6	395.9				
4	1,268	(0,2,0)	570	648.6	659.9				
5	1,301	(0,1,1)	603	696.7	746.4				
6	1,317	(0,0,2)	619	612.3	691.2				
7	1,490	(0,3,0)	792	892.9	879.7				
8	1,548	(0,2,1)	850	998.7					
9	1,586	(0,1,2)	888	956.4					
10	1,661	(0,0,3)	963	923.8					
11	1,668	(0,4,0)	970	1,143.1					
12	1,743	(0,3,1)	1,045	1,189.0					
13	1,802	(0,5,0)	1,104	1,350.0					
14	1,814	(0,2,2)	1,116	1,238.8					
15	1,887	(0,4,1)	1,189	1,411.1					
16	1,896	(0,6,0)	1,198	1,516.2					
17	1,915		1,217			1	1,914	(0,0,0)	0
18	1,925	(0,1,3)	1,227	1,273.4					
19	1,952		1,254			2	1,948	(0,0,1)	34
20	1,966		1,268			3	1,966	(0,1,0)	52
21	1,980		1,282						
22	1,995		1,297						
23	1,997		1,299			4	2,001		87
24	2,003		1,305			5	2,005		91
25	2,025		1,327			6	2,025		111
26	2,030		1,332			7	2,038		124
27	2,043		1,345			8	2,040		126

[a]In this work relative energies are given with respect to the Li + HF dissociation limit. The Li + HF ZPE is 2,045 cm^{-1}_2, the energies of the LiHF $\tilde{X}(1^2A')$ ground electronic state and the Li...HF linear minimum ($^2\Sigma^+$) are −1,706 and −288 cm^{-1}, respectively

[b]Two-dimensional variational results. For details see Table 3 in Ref. [12]

[c]The values are taken from Ref. [9]

[d]The results were obtained in the smaller *R* box. The *R* parameter varied between $6.0a_0$ and $14.0a_0$, with step $0.073a_0$

Anisotropy of the interaction energy contributions

The next goal of this study is to explain the physical origin of the stability of indicated vdW structures in terms of interaction energy contributions calculated using I-PT theory. The decomposition of the SM interaction energies might help us to analyse and estimate how the fundamental components determine its anisotropy.

The UHF interaction energies (ΔE^{UHF}) display a very strong dependence on the angle θ and distance *R*. The contour map shown in Fig. 2b reveals two minima. The first minimum occurs for the geometry corresponding to the global minimum on the PES and the second one appears for the linear arrangement around $R = 5$ Å. This fact indicates that the stability of the first vdW structure is mainly influenced by the contributions included in the ΔE^{UHF} energy. The decomposition of the ΔE^{UHF} energy leads to the ΔE^{HL} (Fig. 3a) and ΔE^{UHF}_{def} (Fig. 4a) terms. The dependence of the terms just mentioned on θ and *R* shows no extremal points in the depicted range.

The consecutive separation of the HL energy according to Eq. (3) reveals that the positive value of this term comes out not only from the repulsive character of the HL exchange-penetration energy contributions (ΔE^{HL}_{exch}), but also from the first-order Hartree–Fock electrostatic energy ($E^{(100)}_{els}$), in certain cases. The repulsive character of Coulomb forces represented by the term $E^{(100)}_{els}$ evidently appears at the hydrogen side of the HF molecule (Fig. 3b). This might be explained by the fact that electrostatic repulsion between lithium and hydrogen nuclei is stronger than the mutual attraction between electrons of the lithium atom and the hydrogen nucleus. However, the shift of the interacting lithium atom toward the fluorine atom leads to the effective increase of electrostatic attraction. The electrostatic border (contour line with $E^{(100)}_{els} = 0$) proceeds from $\theta = 140°$, $R = 2$ Å to the linear arrangement near $R = 4$ Å. We can see that the HL energy in the area of the secondary vdW minimum is influenced only by the ΔE^{HL}_{exch} energy. On the other hand, the strong repulsion of the ΔE^{HL}_{exch} energy around the first minimum is effectively damped by the HF electrostatic contributions.

The UHF deformation term (ΔE^{UHF}_{def}) shows a reciprocal character to the ΔE^{HL} anisotropy (Fig. 4a) and has a dominant stabilisation effect on the total SCF interaction energy around the bent vdW structure. The origin of the large ΔE^{UHF}_{def} energy is quite interesting. The important part of this energy represents the Coulombic induction term ($E^{(200)}_{ind}$) which describes the classic charge induction. As we can see from Table 3, the induction interaction between the neutral lithium atom and the HF molecule in a linear arrangement is about 397 cm^{-1} smaller than for $\theta = 113°$. As Li and HF separate, the relevant exchange-penetration counterpart($E^{(200)}_{exch-ind}$) goes to zero faster than the Coulombic energy $E^{(200)}_{ind}$ (Fig. 4b, c). The strong compensation effects of attractive $E^{(200)}_{ind}$ and repulsive $E^{(200)}_{exch-ind}$ energies indicates that the higher orders of induction energies as well as the response or orbital-relaxation effects play a nonnegligible role in the HF deformation energy [3, 20, 21].

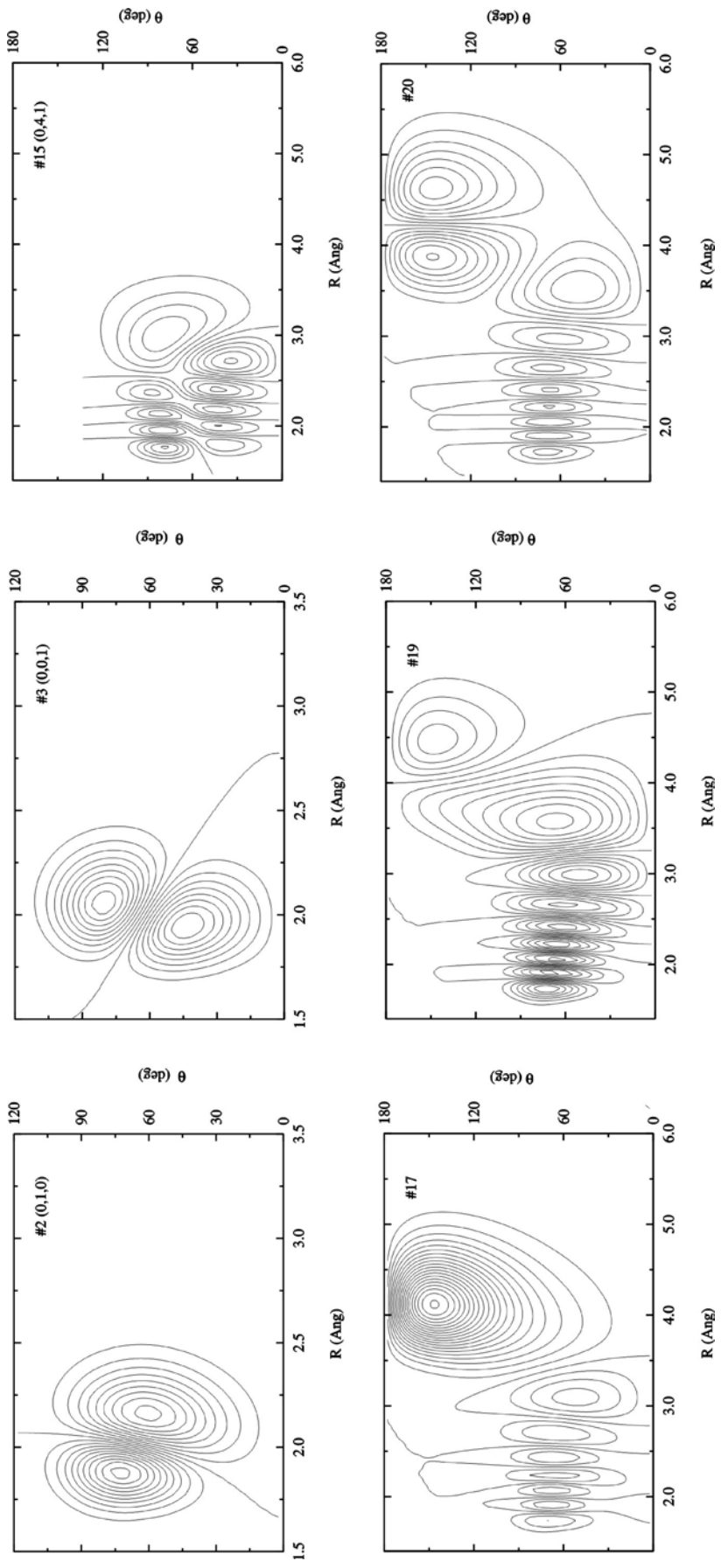

Fig. 1. $J=0$ wave functions for the LiHF $\tilde{\mathbf{X}}(1^2\mathrm{A}')$ ground electronic state with assignments # i (v_r,v_R,v_θ), where i is the number of the state given in Table 4

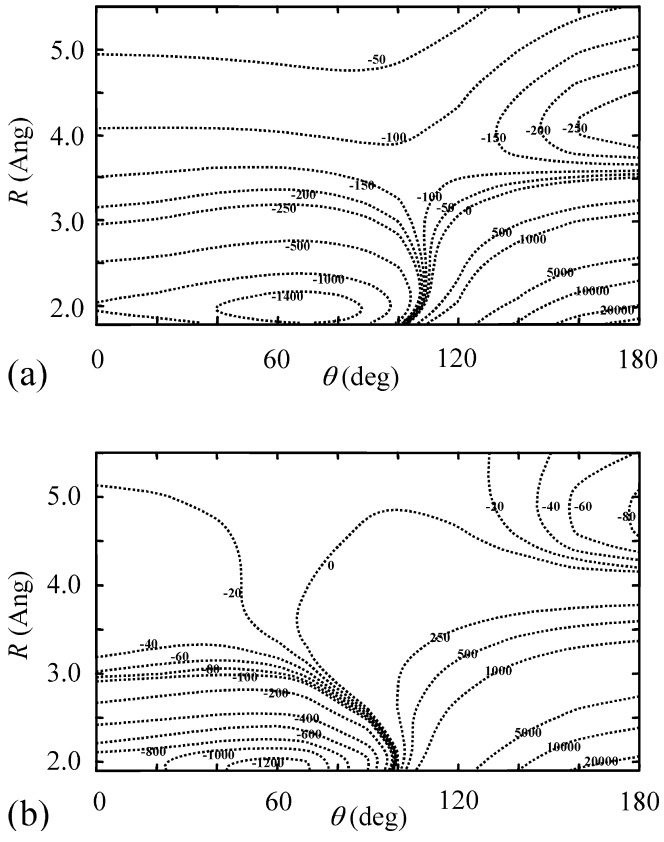

Fig. 2. Contour plots: **a** supermolecular interaction energies calculated at the unrestricted fourth-order Møller–Plesset level of theory ($\Delta E_{\mathrm{int}}^{(4)}$) and **b** supermolecular self-consistent-field interaction energies calculated at the unrestricted Hartree–Fock (*UHF*) level of theory (ΔE^{UHF}). All energies are in cm^{-1}

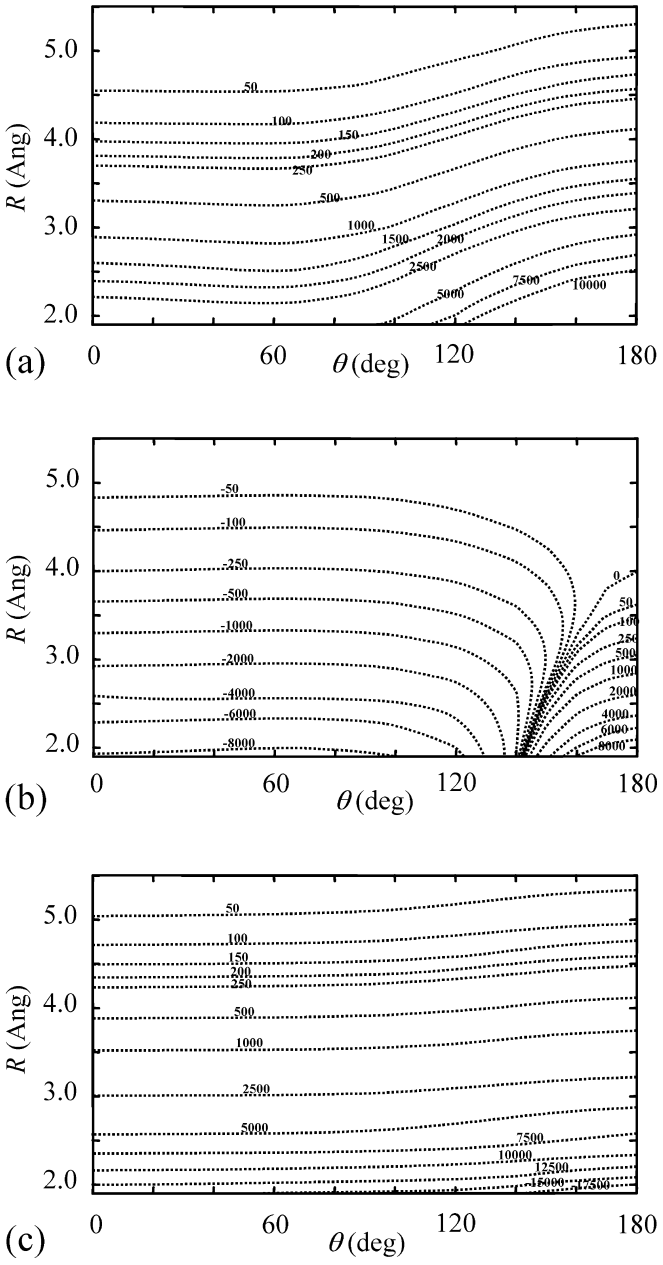

Fig. 3. Contour plots: **a** Heitler–London (*HL*) energies (ΔE^{HL}), **b** first-order Hartree–Fock electrostatic energies ($E_{\mathrm{els}}^{(100)}$) and **c** HL exchange-penetration energies ($\Delta E_{\mathrm{exch}}^{\mathrm{HL}}$). All energies are in cm^{-1}

Similarly, the interaction correlation contributions are important in forming the shape of the total interaction energy curves. $\Delta E^{(2)}$ is determined by dispersion terms $E_{\mathrm{disp}}^{(200)}$ and $E_{\mathrm{exch-disp}}^{(200)}$. Although the $E_{\mathrm{disp}}^{(200)}$ quantities are smaller than $E_{\mathrm{ind}}^{(200)}$ ones, the addition of the exchange-penetration counterparts ($E_{\mathrm{exch-disp}}^{(200)}$ and $E_{\mathrm{exch-ind}}^{(200)}$) indicates comparable importance of dispersion and induction interactions calculated at the second-order level of I-PT (Table 3, Fig. 5). The other calculated attractive but smaller term represents the electrostatic correlation energy ($E_{\mathrm{els}}^{(12)}$). The sum of the exchange-penetration contribution, the deformation energies, and the response effects, $\Delta E_{\mathrm{other}}^{(2)}$, is positive, 1,115.1 cm^{-1}, at $\theta = 70°$, while it is -62.5 cm^{-1} at $\theta = 180°$.

Table 3 (see $E_{\mathrm{disp}} = E_{\mathrm{disp}}^{(200)} + E_{\mathrm{disp}}^{(300)} + E_{\mathrm{disp}}^{(210)} + E_{\mathrm{disp}}^{(201)}$) also provides the higher-order dispersion corrections ($E_{\mathrm{disp}}^{(210)}$, $E_{\mathrm{disp}}^{(201)}$ and $E_{\mathrm{disp}}^{(300)}$) which appear in third-order interaction correlation energy ($\Delta E^{(3)}$). Near the global minimum their sum is positive (131.1 cm^{-1}). It is evident that the sum of the higher-order dispersion corrections does not approximate very well the SM correlation third-order contribution. The sum of the remaining relevant energies (i.e. third-order electrostatic-correlation, exchange-penetration and deformation contributions) seems not to be negligible.

Conclusion

The ab initio PES for the Li(^{2}S)–HF ($\tilde{\mathrm{X}}^1\Sigma^+$) interaction was evaluated at the UMP4 level and analysed by I-PT. The first, relatively deep well ($D_e = 1{,}706$ cm^{-1}) occurs for the bent structure (the FH–Li angle $\theta = 70°$ and $R = 1.95$ Å). The well depth of the secondary minimum

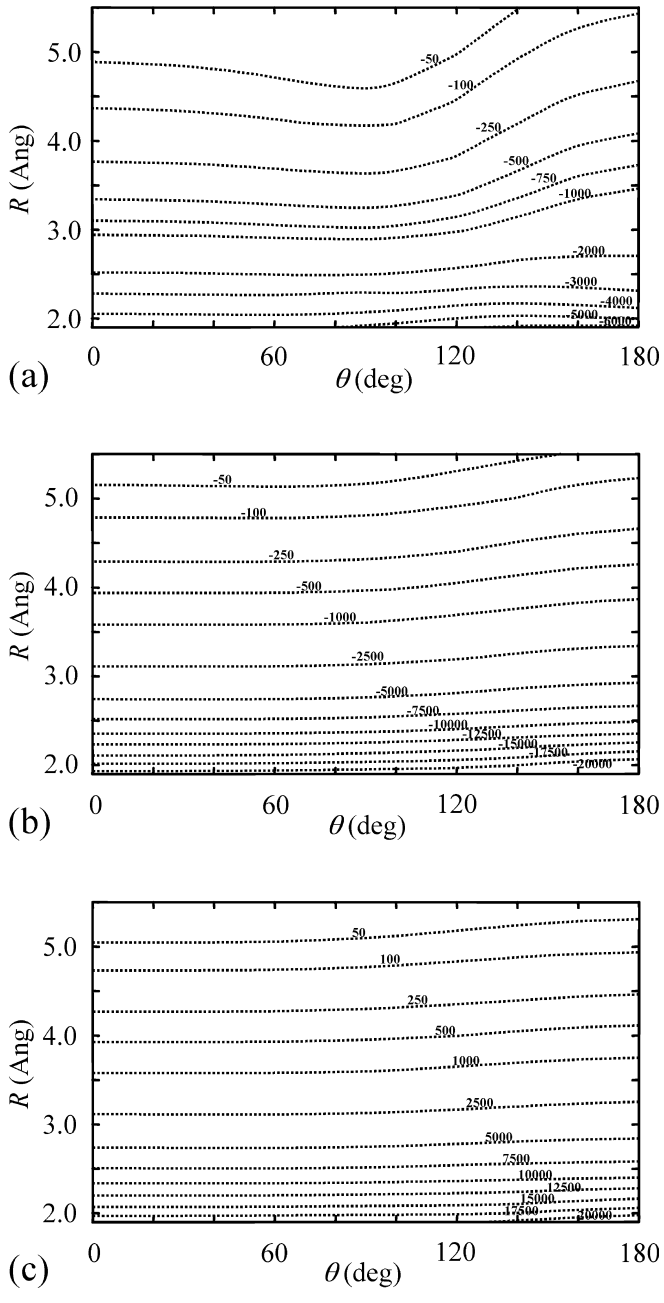

Fig. 4. Contour plots: **a** UHF deformation energies ($\Delta E_{\mathrm{def}}^{\mathrm{UHF}}$), **b** second-order Coulomb induction energies ($E_{\mathrm{ind}}^{(200)}$) and **c** second-order exchange-penetration induction energies ($E_{\mathrm{exch-ind}}^{(200)}$). All energies are in cm^{-1}

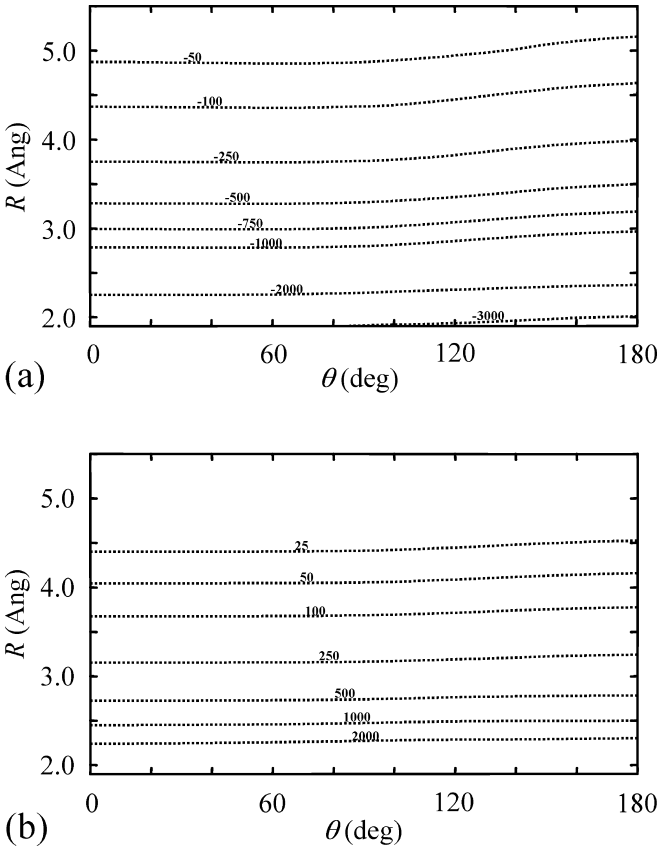

Fig. 5. Contour plots: **a** second-order dispersion energies ($E_{\mathrm{disp}}^{(200)}$) and **b** second-order exchange-penetration dispersion energies ($E_{\mathrm{exch-disp}}^{(200)}$). All energies are in cm^{-1}

is $D_{\mathrm{e}} = 288\ \mathrm{cm}^{-1}$) for the linear arrangements ($\theta = 180°$ and $R = 4.11$ Å). Our results for the global minimum are in good agreement with the previous calculations performed at the MRDCI and CCSD(T) levels of theory. The stability of the vdW minima was investigated by means of the bound-state calculations. We found 27 bound states of the bent Li...FH minimum and eight bound states of the linear Li...HF minimum up to the Li + HF dissociation threshold (2,045 cm^{-1}). While the wave functions for the lowest states of the Li...FH ground electronic state are regular and assignable, the degree of mixing and complexity increases at energies above 1,900 cm^{-1} owing to the presence of the linear vdW minimum. To obtain more precise results, a complex analysis with a nonrigid HF molecule is desirable.

The physical origin of interaction energy anisotropy was evaluated using the four fundamental components, electrostatic, exchange-penetration, induction and dispersion, which have a physical interpretation similar to those arising among the closed-shell species [14, 26]. The analysis of these components reveals that the UHF interaction energies calculated for the bent arrangement are practically determined by the repulsive ΔE^{HL} energies and attractive induction energies included in $\Delta E_{\mathrm{def}}^{\mathrm{UHF}}$ term. The global minimum is stabilised using the attractive Coulombic interaction and UHF deformation energy. The latter term originates from the mutual electric polarisation effects. The secondary linear minimum is mostly determined by the anisotropy of the repulsive HL exchange-penetration ($\Delta E_{\mathrm{exch}}^{\mathrm{HL}}$) and attractive dispersion ($E_{\mathrm{disp}}^{(200)}$) energies.

Acknowledgement. This work was supported by the Slovak Scientific Grant Agency (project nos. 1/0055/03 and 1/0052/03).

References

1. Hobza P, Zahradník (1988) Chem Rev 88:871
2. Chalasiński G, Szczęśniak MM (1994) Chem Rev 94:1723
3. Chalasiński G, Szczęśniak MM (2000) Chem Rev 100:4227
4. Müller-Dethlefs K, Hobza P (2000) Chem Rev 100:143
5. Becker CH, Casavecchia P, Tiedemann PW, Valentini JJ, Lee YT (1980) J Chem Phys 73:2833
6. Loesh HJ, Stienkemeier F (1993) J Chem Phys 98:9570
7. Loesh HJ, Stienkemeier F (1993) J Chem Phys 99:9598
8. Hudson AJ, Oh HB, Polanyi JC (2000) J Chem Phys 113:9897
9. Paniagua M, Aguado A, Lara M, Roncero O, Piecuch P (1999) J Chem Phys 111:6712
10. Aguado A, Paniagua M, Lara M, Roncero O (1997) J Chem Phys 107:10085
11. Jasper AW, Hack MD, Chakraborty A, Truhlar DG (2001) J Chem Phys 115:7946
12. Burcl R, Piecuch P, Špirko V, Bludský O (2000) Int J Quantum Chem 80:916
13. van Duijneveldt FB, van Duijneveldt- van de Rijdt JGCN, van Lenthe JH (1994) Chem Rev 94:1873
14. Cybulski SM, Kendall RA, Chalasiński G, Severson MW, Szczęśniak MM (1997) J Chem Phys 106:7731, and references therein
15. Lukeš V, Laurinc V, Biskupič S (1999) J Comput Chem 20:857
16. Lukeš V, Bittererová M, Laurinc V, Biskupič S (2000) Chem Phys 257:157, and references therein
17. Lukeš V, Vrábel I, Laurinc V, Biskupič S (2001) J Phys Chem A 105:7686, and references therein
18. Löwdin P-O (1956) Adv Phys 5:1
19. Lukeš V, Laurinc V, Biskupič S (1999) Int J Quantum Chem 20:857, and references therein
20. Jeziorski B, Moszyński R, Ratkiewicz A, Rybak, S, Szalewicz K, Williams HL (1993) In: Clementi E (ed) Methods and techniques in computational chemistry: METECC-94 vol B. STEF, Cagliari, pp 79–129
21. Jeziorski B, van Hemert NC (1976) Mol Phys 31:713
22. Kochanski E (1973) J Chem Phys 58:5823
23. Frisch MJ, Trucks GW, Schlegel HB, Gill PMW, Johnson BG, Robb MA, Cheeseman JR, Keith T, Petersson GA, Montgomery JA, Raghavachari K, Al-Laham MA, Zakrzewski VG, Ortiz JV, Foresman JB, Cioslowski J, Stefanov BB, Nanayakkara A, Challacombe M, Peng CY, Ayala PY, Chen W, Wong MW, Andres JL, Replogle ES, Gomperts R, Martin RL, Fox DJ, Binkley JS, Defrees DJ, Baker J, Stewart JP, Head-Gordon M, Gonzalez C, Pople JA (1995) Gaussian 94. Gaussian, Pittsburgh, PA
24. Boys SF, Bernardi F (1970) Mol Phys 19:553
25. Dunning TH Jr (1989) J Chem Phys 90:1007
26. Kendall RA, Dunning TH Jr, Harrison RJ (1992) J Chem Phys 96:6796
27. Sadlej AJ (1988) Collect Czech Chem Commun 53:1995
28. Goldfield EM, Gray SK, (1996) Comput Phys Commun 98:1
29. Yang C-Y, Gray SK (1997) J Chem Phys 107:7773
30. Nanbu S, Gray SK, Kinoshita T, Aoyagi M (2000) J Chem Phys 112:5866
31. Delgado-Barrio G (1993) In: Delgado-Barrio G (ed) Dynamical processes in molecular physics. IOP, Bristol, pp 219–248
32. Huber KP, Herzberg G (2001) In: Linstrom PJ, Mallard WG (eds) NIST chemistry webbook. NIST standard reference database no. 69, July 2001. National Institute of Standards and Technology, Gaithersburg, http://webbook.nist.gov
33. Lill JV, Parker GA, Light JC (1982) Chem Phys Lett 89:483
34. Colbert DT, Miller WH (1992) J Chem Phys 96:1982
35. Echave J, Clary DC (1992) Chem Phys Lett 190:225
36. Wei H, Carrington T (1992) J Chem Phys 97:3029
37. ARPACK users' guide: Solution of large scale eigenvalue problems with implicitly restarted Arnoldi methods. (1997) Rice University
38. Engels-Müllges G, Uhlig F (1996) Numerical algorithms with FORTRAN. Springer, Berlin Heidelberg New York
39. Chen MML, Schaefer HF III (1980) J Chem Phys 72:4376